NEOPLASIA
www.neoplasia.com

Volume 12 Number 1 January 2010 pp. 80–86 80

Activation of the Unfolded Protein Response Contributes toward the Antitumor Activity of Vorinostat[1]

Soumen Kahali[*,†], Bhaswati Sarcar[*,†], Bin Fang[‡], Eli S. Williams[§], John M. Koomen[‡,¶], Philip J. Tofilon[§] and Prakash Chinnaiyan[*,†]

*Radiation Oncology, H. Lee Moffitt Cancer Center, Tampa, FL, USA; [†]Experimental Therapeutics, H. Lee Moffitt Cancer Center, Tampa, FL, USA; [‡]Proteomics, H. Lee Moffitt Cancer Center, Tampa, FL, USA; [§]Drug Discovery, H. Lee Moffitt Cancer Center, Tampa, FL, USA; [¶]Molecular Oncology, H. Lee Moffitt Cancer Center, Tampa, FL, USA

Abstract

Histone deacetylase (HDAC) inhibitors represent an emerging class of anticancer agents progressing through clinical trials. Although their primary target is thought to involve acetylation of core histones, several nonhistone substrates have been identified, including heat shock protein (HSP) 90, which may contribute towards their antitumor activity. Glucose-regulated protein 78 (GRP78) is a member of the HSP family of molecular chaperones and plays a central role in regulating the unfolded protein response (UPR). Emerging data suggest that GRP78 is critical in cellular adaptation and survival associated with oncogenesis and may serve as a cancer-specific therapeutic target. On the basis of shared homology with HSP family proteins, we sought to determine whether GRP78 could serve as a molecular target of the HDAC inhibitor vorinostat. Vorinostat treatment led to GRP78 acetylation, dissociation, and subsequent activation of its client protein double-stranded RNA-activated protein-like endoplasmic reticulum kinase (PERK). Investigations in a panel of cancer cell lines identified that UPR activation after vorinostat exposure is specific to certain lines. Mass spectrometry performed on immunoprecipitated GRP78 identified lysine-585 as a specific vorinostat-induced acetylation site of GRP78. Downstream activation of the UPR was confirmed, including eukaryotic initiating factor 2α phosphorylation and increase in ATF4 and C/EBP homologous protein expression. To determine the biologic relevance of UPR activation after vorinostat, RNA interference of PERK was performed, demonstrating significantly decreased sensitivity to vorinostat-induced cytotoxicity. Collectively, these findings indicate that GRP78 is a biologic target of vorinostat, and activation of the UPR through PERK phosphorylation contributes toward its antitumor activity.

Neoplasia (2010) 12, 80–86

Introduction

Although cancer has traditionally been considered a disease originating from genetic alterations resulting in functional loss of tumor-suppressor genes or gain of oncogenes, epigenetic modifications, or modulating gene expression through mechanisms other than changes in the underlying DNA sequence have emerged as a contributing factor toward oncogenesis [1]. Regulating gene expression through histone acetylation represents a form of epigenetic modification. Histones comprise the protein backbone of chromatin, and in the acetylated state, the chromatin is in an open configuration, allowing accessibility for specific transcription factors and/or the general transcription machinery [2]. The opposing activities of histone acetyltransferases and histone deacetylases (HDACs)

Abbreviations: ATF, activated transcription factor; CHOP, C/EBP homologous protein; eIF, eukaryotic initiation factor; GRP78, glucose-regulated protein 78; HSP, heat shock protein; HDAC, histone deacetylase; PERK, double-stranded RNA-activated protein-like endoplasmic reticulum kinase; UPR, unfolded protein response

Address all correspondence to: Prakash Chinnaiyan, MD, H. Lee Moffitt Cancer Center and Research Institute, SRB3, 12902 Magnolia Dr, Tampa, FL 33612.
E-mail: prakash.chinnaiyan@moffitt.org

[1]This work was supported in part by the Miles for Moffitt Research Award (P.C.). The Moffitt Proteomics Facility is supported by the US Army Medical Research and Material Command under Award No. DAMD17-02-2-0051 for a National Functional Genomics Center, the National Cancer Institute under Award No. P30-CA076292 as a Cancer Center Support Grant, and the Moffitt Foundation.
Received 18 August 2009; Revised 8 October 2009; Accepted 8 October 2009

DOI 10.1593/neo.91422

result in histone acetylation and deacetylation, respectively, leading to chromatin remodeling and transcriptional regulation.

Currently, it is widely recognized that HDACs represent promising therapeutic targets, with an underlying rationale of reversing aberrant epigenetic states associated with cancer. For example, both aberrant recruitment of HDACs to promoter regions and altered expression of HDACs have been reported in several tumor types [3,4]. Consequently, there has been considerable effort in the development of HDAC inhibitors as a form of targeted anticancer therapy. A large number of structurally diverse HDAC inhibitors have been identified demonstrating preclinical activity in various cancer cell lines [4–6]. Several are currently in clinical evaluation, including valproic acid and vorinostat (suberoylanilide hydroxamic acid; Zolinza), which is an HDAC inhibitor that has recently been granted Food and Drug Administration approval for use in cutaneous T-cell lymphoma and is currently being tested in solid tumors.

Although reversal of aberrant epigenetic changes has been considered the primary mechanism underlying HDAC inhibitor antitumor activity, recent investigations suggest their effects may be considerably broader, largely based on the expanding number of recently identified nonhistone substrates of HDACs. At least 50 nonhistone proteins of known biologic function have been identified, suggesting a more appropriate term for these enzymes may be *protein* rather than *histone* deacetylases [3,4]. These nonhistone protein targets include transcription factors, chaperone proteins, DNA repair proteins, and structural proteins, and acetylation can either increase or decrease their function or stability. As these identified HDAC substrates are involved in a diverse array of biologic processes, multiple mechanisms may influence the activity of HDAC inhibitors.

A specific nonhistone target of HDAC inhibitors that has gained recent attention is the chaperone protein heat shock protein 90 (HSP90). HSP90 is required for the stability and function of numerous client proteins, including mutated and overexpressed proteins that promote cancer cell growth and survival, suggesting its potential to serve as a therapeutic target [7]. Recent investigations demonstrated the potential of HDAC inhibitors to acetylate HSP90, leading to dissociation of its client oncoproteins, including ErbB1, ErbB2, bcr-abl, and Akt. Further investigations identified HDAC6 as the putative target [8,9] and acetylation to play a functional role in regulating the HSP90 chaperone cycle [7]. Although HDAC inhibitors have demonstrated the capacity to influence HSP90 acetylation, it remains unclear the degree to which this influences their antitumor activity.

In this report, we identified the endoplasmic reticulum (ER) chaperone protein glucose-regulated protein 78 (GRP78) to serve as another nonhistone target of HDAC inhibitors. GRP78, which shares close homology with the heat shock family of proteins, serves as the critical sensor for ER stress and as an activator of the unfolded protein response (UPR), a highly specific signaling pathway to cope with the accumulation of unfolded or misfolded proteins [10,11]. Recent investigations suggest that GRP78 may be an important mediator in maintaining survival in "stressed" cells, such as cancer, and therefore may have therapeutic implications [12]. We have shown that GRP78 is acetylated after HDAC inhibition, leading to dissociation of its client protein double-stranded RNA-activated protein-like ER kinase (PERK), activation of the UPR, and abrogating this pathway leads to decreased sensitivity to vorinostat-induced cytotoxicity. Collectively, these findings indicate that GRP78 is a biologic target of HDAC inhibitors, and activation of the UPR through PERK phosphorylation contributes toward its antitumor activity.

Materials and Methods

Cell Lines and Treatment

Cell lines were obtained from the National Cancer Institute Frederick Tumor Repository. Cells were maintained in RPMI medium supplemented with either 5% (U251, DU145, or SF539) or 10% (U87 or PC3) fetal bovine serum and glutamate (5 mM). Cell cultures were maintained at 37°C and 5% CO_2. Vorinostat was provided by Merck Research Laboratories (Whitehouse Station, NJ) through the NCI-CTEP and was dissolved in DMSO at 1 mM. Valproic acid was purchased from Sigma-Aldrich (St. Louis, MO) and dissolved in PBS at 100 mM.

Immunoprecipitation

Cellular extracts were prepared with lysis buffer (50 mM Tris-HCl [pH 7.4], 150 mM NaCl, 1 mM EDTA, 0.5% Na-deoxycholate, 0.7 μg/ml pepstatin, 1% NP-40, and protease inhibitor cocktail). Five hundred micrograms of whole-cell lysates was precleared with a 50-μl mixture of protein A-agarose and protein G-agarose (Roche Diagnostic Corp., Indianapolis, IN) in a rotator at 4°C overnight. Fifteen micrograms of rabbit GRP78 polyclonal primary antibody (Santa Cruz Biotechnology, Santa Cruz, CA) was added to the lysate and incubated for 3 hours at 4°C. Then, 50 μl of protein A-agarose beads was added to the lysate and incubated overnight at 4°C. Beads were then pelleted by centrifugation and washed three times with 1) ice-cold washing buffer, 2) high salt buffer (50 mM Tris-HCl [pH 7.4], 500 mM NaCl, 1 mM EDTA, 0.05% sodium deoxycholate, 0.1% NP-40, and protease inhibitor cocktail [Roche Diagnostic Corp.]), and (3) low salt buffer (50 mM Tris-HCl [pH 7.4], 1 mM EDTA, 0.05% sodium deoxycholate, 0.1% NP40, and protease inhibitor cocktail [Roche Diagnostic Corp.]). Pellet was then resuspended in sample buffer, heated at 90°C for 10 minutes, and centrifuged.

Immunoblot Analysis

For the extraction of the whole-cell lysates, cells were harvested by centrifugation at 1000 rpm for 5 minutes. Cell pellets were washed once with PBS, gently resuspended in 200 μl of lysis buffer (1% Triton X-100, 1 mM phenylmethylsulfonyl fluoride, 10 μg/ml leupeptin, 1 μg/ml pepstatin-A, 2 μg/ml aprotinin, 20 mM *p*-nitrophenyl phosphate, 0.5 mM sodium orthovanadate, 1 mM 4-(2-aminoethyl) benzenesulfonylfluoride hydrochloride) with protease inhibitor cocktail (Roche Diagnostic Corp.) and phosphatase inhibitor (Sigma-Aldrich), and incubated on ice with occasional vortexing for 30 minutes. Cell lysates were centrifuged at 12,000 rpm in a tabletop centrifuge for 15 minutes to remove the nuclear and cellular debris. Proteins were resolved by sodium dodecyl sulfate–polyacrylamide gel electrophoresis (SDS-PAGE), transferred to polyvinylidene difluoride (PVDF) membranes (Millipore, Billerica, MA), blocked with 5% milk, and incubated with primary antibody. Primary antibodies used include anti–acetyl lysine, anti–total eukaryotic initiating factor 2α (eIF2α) and anti–eIF2α Ser51 phosphospecific antibody (Cell Signaling Technology, Beverly, MA), anti–phosphospecific PERK, anti-PERK, anti-ATF4, anti–C/EBP homologous protein (CHOP), and anti-GRP78 (Santa Cruz Biotechnology), and antiactin (Sigma-Aldrich). Secondary antibodies conjugated to horseradish peroxidase (Santa Cruz Biotechnology) were used, and chemiluminescence (Thermo Fisher Scientific, Rockford, IL) or enhanced chemiluminescence (GE Healthcare, Piscataway, NJ) was used for detection.

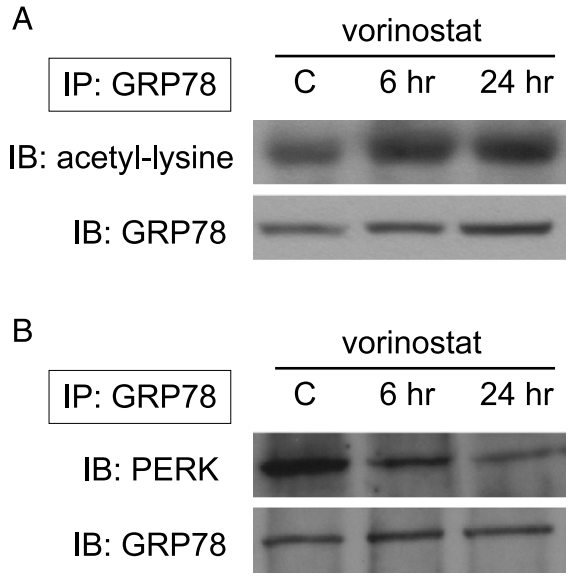

Figure 1. HDAC inhibition with vorinostat leads to GRP78 acetylation and dissociation with its client protein PERK. The glioblastoma cell line U251 was exposed to vorinostat (1 μM) for 6 and 24 hours. Cell lysates were immunoprecipitated (IP) for GRP78 and immunoblot (IB) was performed for (A) acetyl-lysine and (B) PERK. IB for GRP78 served as loading control.

Liquid Chromatography Coupled with Tandem Mass Spectrometry

For the detection of discrete acetylation sites of GRP78, liquid chromatography coupled with tandem mass spectrometry (LC–MS/MS) was used. Immunoprecipitated GRP78 was resolved on 4% to 15% gradient gel (Bio-Rad, Hercules, CA) using SDS-PAGE. Gel bands corresponding to GRP78 were excised and washed once with water and twice with 50-mM ammonium bicarbonate in 50% aqueous methanol. After reduction with triscarboxyethyl phosphine and alkylation with iodoacetamide, samples are digested overnight with modified sequencing grade trypsin (Promega, Madison, WI). Peptides were extracted from the gel slices and concentrated under vacuum centrifugation. A nanoflow liquid chromatograph (U3000; Dionex, Sunnyvale, CA) coupled to an electrospray ion trap mass spectrometer (LTQ Orbitrap; Thermo, San Jose, CA) was used for tandem mass spectrometry peptide sequencing experiments. Peptides were separated with a C18 reverse phase column (75-µm inner diameter × 15 cm, C18Pepmap; Dionex) using a 90-minute gradient from 5% to 50% B (A: 2% acetonitrile/0.1% formic acid; B: 90% acetonitrile/0.1% formic acid). Five tandem mass spectra were acquired for each MS scan (spray voltage, 2.5 kV; 30% normalized collision energy; scanning *m/z*, 450-1600). Sequences were assigned using SEQUEST (Thermo) and Mascot (www.matrixscience.com) database searches against SwissProt human protein entries. In addition to acetylysine, oxidized

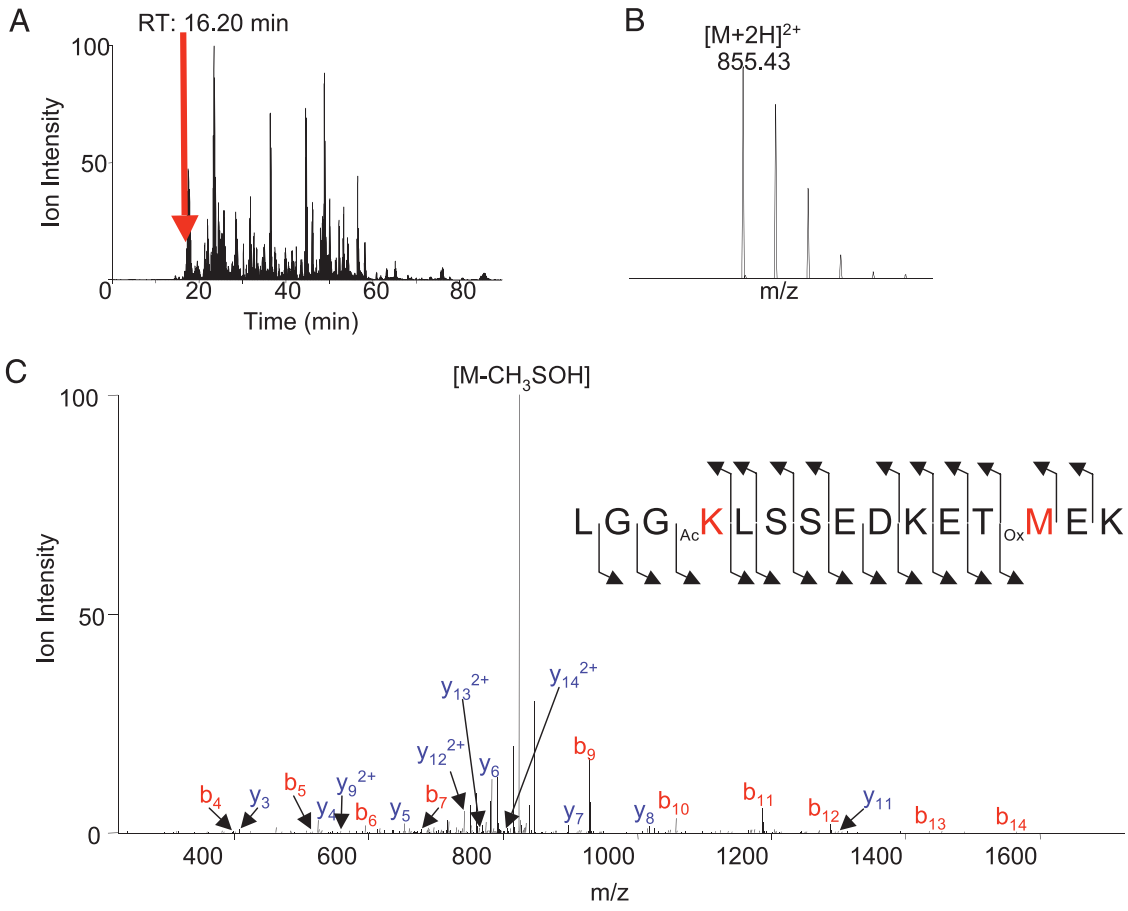

Figure 2. GRP78 acetylation assessed in U251 cells treated with vorinostat (1 μM, 24 hours) and vehicle control using LC–MS/MS. The peptide was detected at 16.20 minutes in the total ion chromatogram (A) with a mass-to-charge ratio of 855.4332 (B). The tandem mass spectrum matched the sequence, (K)LGG$_{Ac}$**K**LSSEDKET$_{Ox}$MEK(A), indicating increased lysine-585 acetylation in vorinostat treated cells; the detection of y_{11} and y_{12} is consistent with this localization (C). The assignment was made with MASCOT with an ion score 35.8; SEQUEST XCorr 2.30 ΔC_n 0.15.

methionine, deamidation, and carbamidomethyl cysteine were selected as variable modifications, and as many as three missed cleavages were allowed. Assignments were manually verified by inspection of the tandem mass spectra and coalesced into Scaffold reports (www.proteomesoftware.com). The integrated peak areas for peptide quantification were calculated from extracted ion chromatograms using QuanBrowser from Xcalibur 2.0. These values were restricted by *m/z* (±0.02) and retention time (120 seconds). The masses and isotopic peak patterns of the target peptides were manually inspected to ensure proper sequence assignment and to verify peak quality. The signal intensities from unmodified GRP78 peptides were used to normalize the amount of protein introduced into mass spectrometer.

Protein Synthesis

U251 cells were seeded in six-well plates and allowed to adhere overnight. Cells were then treated with vorinostat or vehicle control (DMSO) for the described periods. Before collection, cells were starved in methionine- and cysteine-free medium for 1 hour and radiolabeled with 50 μCi/ml [^{35}S]-methionine (specific activity, 1175.0 Ci/mmol) Easytag Express Protein labeling mix [^{35}S] (PerkinElmer, Waltham, MA) for 40 minutes. As a positive control, an untreated culture was exposed to cycloheximide (50 μg/ml) at the time of methionine/cysteine–free medium addition. Medium was aspirated, and cells were lysed by adding 1% Triton X-100 in 50 mM Tris (pH 7.5), 2 mM EDTA, and 1 mM dithiothreitol. Trichloroacetic acid (TCA) precipitation of macromolecules and scintillation counting were performed as follows: 20 μl of cell lysate was added to 60 μl of 20% TCA in water (vol./vol.). The samples were kept on ice for 1 hour and then filtered through glass filters (GF/C filters; Whatman, Piscataway, NJ) under vacuum. The filter was washed three times with ice-cold TCA (10%, vol./vol.) followed by one wash in 95% ethanol and then immersed in 5 ml of EcoLume Liquid Scintillation Fluid (MP Biomedicals, Solon, OH). Disintegrations per minute were measured on a Beckman LS6500 scintillation counter (Beckman Coulter, Brea, CA), and results were normalized as the percent increase or decrease of [^{35}S]-methionine incorporation compared with that of untreated control cells.

Small Interfering RNA

U251 cells were seeded at 1×10^5 cells per well in six-well plates and allowed to reach 70% confluence on the day of transfection. The small interfering RNA (siRNA) constructs (siGENOME SMARTpool PERK [M-004883-03-0010], siControl nontargeting siRNA pool [D-001206-13-20], and siGENOME SMARTpool reagents) were purchased from Dharmacon (Lafayette, CO). Cells were transfected with 50 nM siRNA in Opti-Mem medium (Invitrogen Life Technologies, Carlsbad, CA) with 5% FCS according to manufacturer's protocol. Forty-eight hours after transfection, cells were trypsinized and plated for clonogenic survival, and the remaining cells were used for Western blot.

Clonogenic Survival

Cells were seeded as single cells in six-well plates and allowed to adhere for 6 hours, treated with vorinostat (1 mM) or vehicle control (DMSO) for 48 hours, then medium was replaced with drug-free medium, and cells were allowed to incubate for 10 to 14 days. Plates were then stained with crystal violet, and colonies consisting of 50 or more cells were manually counted. Results were normalized to the colony-forming efficiency of the vehicle control.

Statistical Analysis

The statistical analysis was done using a Student's *t* test. A probability level of $P < 0.05$ was considered significant. Data are presented as mean ± SD from three independent experiments.

Results

GRP78 Is a Molecular Target of the HDAC Inhibitor Vorinostat

Because the ER chaperone protein GRP78 is a member and shares close homology with the heat shock family of proteins, a previously described target of HDAC inhibitors [3,8,13], we sought to determine whether GRP78 could also be modulated by HDAC inhibition. Initial studies focused on U251, a glioblastoma cell line that has been previously described to both aberrantly express and be reliant on GRP78 for

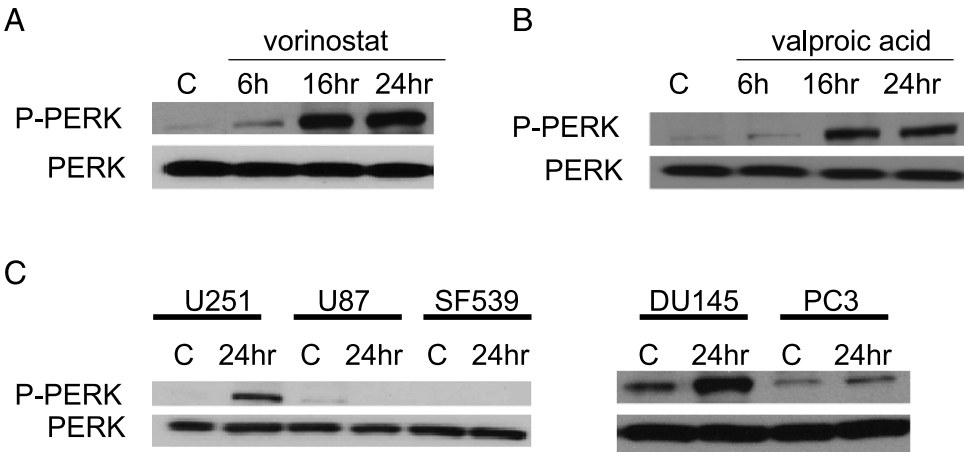

Figure 3. HDAC inhibitors activate the UPR. Western blot was performed on U251 cells in a time course manner to determine whether HDAC inhibitors from disparate molecular classes can activate PERK (P-PERK), a key signaling pathway associated with the UPR. The HDAC inhibitors used include (A) the hydroxamic acid vorinostat (1 μM) and (B) the short-chain fatty acid valproic acid (2.5 mM). (C) Glioblastoma (U251, U87, SF539) and prostate cancer (DU145, PC3) cell lines were treated with vorinostat (1 μM) or vehicle control for 24 hours. Western blot was performed on cell lysates to evaluate for activated PERK (P-PERK).

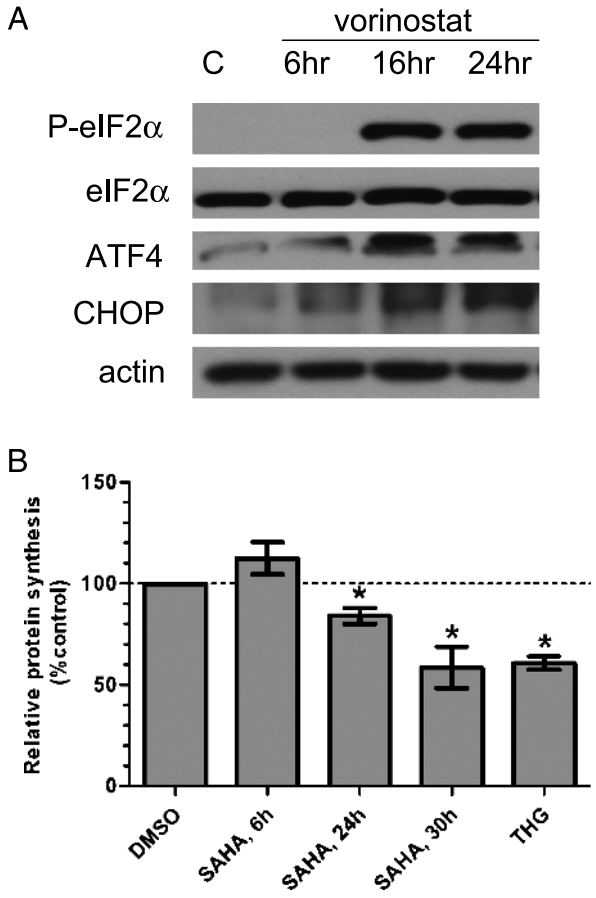

Figure 4. Vorinostat activates downstream signaling of the UPR. (A) Western blot was performed to evaluate activated eIF2α (P-eIF2α), translational up-regulation of ATF4, and CHOP expression in U251 cells after vorinostat exposure. (B) Cells were treated with vorinostat (SAHA) for indicated times or thapsigargin (THG, positive control) for 24 hours and exposed to methionine/cysteine–free medium. Cells were then radiolabeled with [^{35}S]-methionine, and protein lysates were collected after 40 minutes. Counts per minute were measured, adjusted for protein concentration, and normalized to the DMSO control. *Columns*, mean; *bars*, SD. *$P < .001$ *versus* control by Student's *t* test.

its continued proliferation [12]. U251 cells were exposed to a clinically relevant concentration of vorinostat (1 μM) [14] or vehicle control in a time course manner. Cell lysates were then immunoprecipitated for GRP78 followed by immunoblot analysis with an antibody that recognizes anti–acetylated lysine residues. As shown in Figure 1*A*, GRP78 is acetylated after 6 and 24 hours of exposure to vorinostat. We next sought to determine whether vorinostat-induced GRP78 acetylation could have a functional consequence of dissociation with its client proteins, the central process involved in UPR activation. Of the known client proteins associated with GRP78, our initial investigations focused on the PERK. As demonstrated in Figure 1*B*, GRP78 dissociates with its client protein PERK in a time course manner consistent with protein acetylation after vorinostat exposure. In addition to GRP78 acetylation and PERK dissociation, both studies demonstrate a modest increase in GRP78 expression after vorinostat exposure, which represents a recognized downstream signaling consequence of UPR activation [10].

As acetylation of GRP78 has not been previously described, we went on to define the specific acetylation sites using LC–MS/MS. Immunoprecipitated GRP78 from U251 cells exposed to vorinostat (1 μM) for 24 hours or vehicle control was separated on SDS-PAGE, and the band identified by molecular weight as GRP78 was excised. In-gel tryptic digestion was performed, and the extracted peptides were analyzed by LC–MS/MS. A nanoflow liquid chromatograph (U3000; Dionex) coupled to an electrospray ion trap mass spectrometer (LTQ Orbitrap; Thermo) was used for tandem mass spectrometry peptide sequencing experiments. Overall, 74% of the GRP78 protein sequence was detected by LC–MS/MS from tryptic digests. To further evaluate our ability to localize acetylation sites, 35 (57%) of 61 lysine residues were contained in peptides sequenced in these experiments. As demonstrated in Figure 2, we identified lysine-585 of GRP78 to be a specific site of acetylation after 24 hours of exposure to vorinostat. Using extracted ion chromatograms for eight peptides, the expression of GRP78 was observed to increase 2.8 ± 1.0-fold after treatment. These results are consistent with immunoblot experiments (Figure 1), suggesting downstream activation of the UPR. Overall, the signal for the acetylated peptide containing lysine-585 was increased by a factor of 4 after treatment. After normalization for GRP78 expression, which was increased after vorinostat exposure (consistent with our previous studies), acetylation on lysine-585 increased an average of 1.5-fold in two biologic replicates after 24 hours of exposure to vorinostat.

HDAC Inhibition Leads to Activation of the UPR

As dissociation of PERK from its chaperone protein GRP78 leads to PERK dimerization and autophosphorylation, a hallmark of the UPR, Western blot was performed to determine whether HDAC inhibitors have the capacity to activate the UPR signaling cascade. Figure 3*A* demonstrates PERK phosphorylation in a time course manner after exposure to vorinostat (1 μM), with maximal activation between 16 and 24 hours, consistent with the above-described GRP78 acetylation and PERK dissociation. Similar findings were observed with the HDAC inhibitor valproic acid using an equitoxic drug concentration (Figure 3*B*), suggesting UPR activation after HDAC inhibition is not agent-specific. To determine whether UPR activation after HDAC inhibition is specific to U251, experiments were expanded to a panel of glioblastoma and prostate cancer cell lines. Although UPR activation was not present in all cell lines tested, it was shown in the prostate cancer cell lines DU145 and, to a lesser extent, PC3, confirming this biologic process was not specific to U251 (Figure 3*C*). Mechanisms underlying disparate UPR activation between cell lines remain unclear.

A primary goal of PERK activation involves reducing the workload on the ER by inhibiting protein biosynthesis, which is accomplished principally through phosphorylation of the alpha subunit of eIF2α and selective expression of activated transcription factor 4 (ATF4). When eIF2α is phosphorylated, the formation of the ternary translation initiation complex eIF2/GTP/Met-tRNA$_i^{Met}$ is prevented, leading to a generalized attenuation of translation and protein synthesis. In addition to a generalized decrease in protein synthesis, phosphorylated eIF2α selectively promotes translation of ATF4, which subsequently activates transcription of genes involved in amino acid metabolism and transport, oxidation-reduction reactions, and ER stress–induced apoptosis [10,15]. As shown in Figure 4*A*, eIF2α is phosphorylated after HDAC inhibition in a time course manner consistent with PERK activation. The functional consequence of eIF2α phosphorylation after HDAC inhibition was also confirmed, with increased ATF4 expression (Figure 4*A*) and decrease in overall protein synthesis determined by *S*-methionine incorporation (Figure 4*B*).

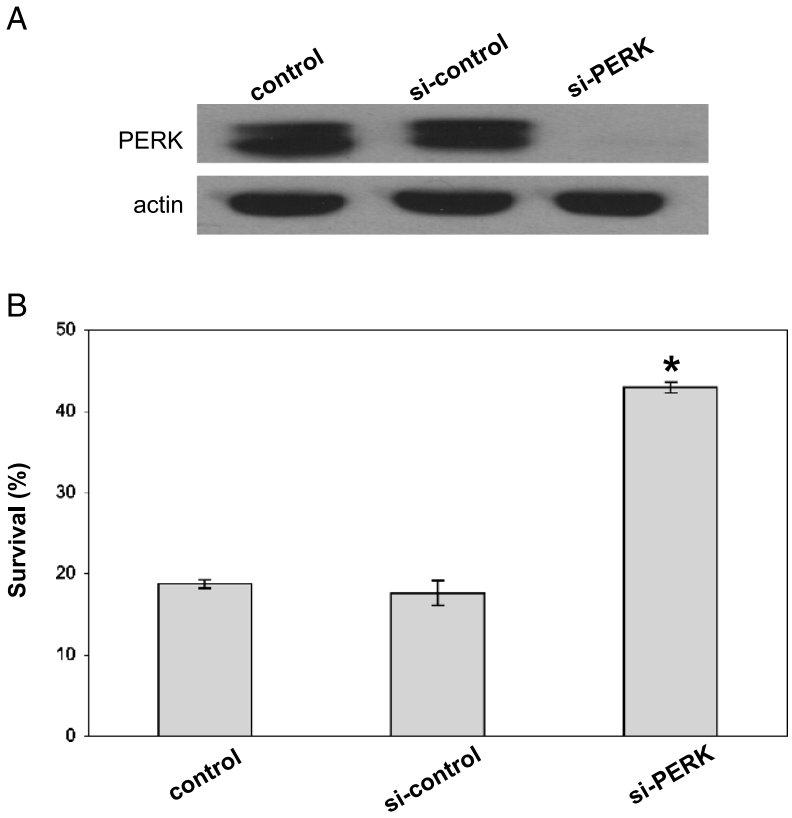

Figure 5. PERK signaling influences vorinostat-induced cytotoxicity. U251 cells were untransfected (control) or transfected with scrambled siRNA (si-control) and siRNA PERK (si-PERK) for 48 hours. (A) Western blot was performed demonstrating successful PERK knockdown. (B) The remainder of the cells were seeded in six-well plates, placed in the incubator for 6 hours to allow to attach, treated with vorinostat (1 μM) or vehicle control for 48 hours, replaced with fresh media, and then allowed to grow for 10 to 14 days. Percent survival was normalized to the colony-forming efficiency of the untreated (vehicle control) cells. *Columns*, mean; *bars*, SD. *$P < .05$ according to Student's *t* test (si-PERK *vs* control and si-PERK *vs* si-control).

Although the primary effects of UPR activation are designed for cellular protection, they may also serve to limit damage to other organelles and can ultimately protect the organism by eliminating cells experiencing prolonged or severe ER stress. Under such conditions, ATF4 induces the transcription factor CHOP, which plays a central role in mediating cell death pathways associated with the UPR [10]. As demonstrated in Figure 4*A*, CHOP expression is increased in a time course manner after vorinostat exposure, suggesting that this pathway contributes toward vorinostat-induced cytotoxicity. To test this more directly, we abrogated this pathway using RNA interference to determine the influence of UPR activation on the antitumor activity of vorinostat. Of the possible proteins involved in this signaling cascade, we chose to focus on PERK because it is a key upstream mediator of pathway activation. Western blot confirmed successful PERK knockdown (Figure 5*A*). When compared with both untransfected U251 (control) and those transfected with scrambled siRNA (si-control), U251 transfected with siPERK demonstrates a nearly two-fold increase in clonogenic survival after vorinostat exposure (Figure 5*B*), supporting the contributory role of this pathway in vorinostat-induced cytotoxicity.

Discussion

Recent scientific advancements in our understanding of UPR activation and its primary regulator GRP78 suggest the critical role this adaptive pathway may play in cancer development and therapeutic resistance [13]. Our findings demonstrate GRP78 to be a nonhistone target of the HDAC inhibitor vorinostat. The localization and function of HDACs within the ER have not been previously described. Therefore, it would be of considerable interest to identify the specific HDAC(s) and histone acetyltransferases involved in GRP78 deacetylation/acetylation to determine their role in UPR activation. In addition, as our data suggest that this process influences vorinostat activity, such studies would provide the rationale for the development of isotype-specific HDAC inhibitors as a strategy for anticancer therapy.

It remains unclear if and how acetylation of GRP78 leads to client protein dissociation. However, the potential for a direct interaction is supported by work involving HSP90, in which protein acetylation/deacetylation was shown to play in integral role in regulating the chaperone cycle by decreasing client protein affinity [7]. In our studies, we identified lysine-585 as a specific GRP78 residue acetylated after vorinostat exposure. Because approximately 57% of the lysine residues could be sequenced with the described methodologies, it remains unknown if other acetylation sites exist within GRP78. However, the degree of GRP78 acetylation after vorinostat exposure determined by mass spectrometry, a 4- and 1.5-fold increase in overall GRP78 acetylation and when normalized for protein expression, respectively, is in accord with our Western blot results. Future studies involving mutational analysis of individual acetylation sites within GRP78 will help to more definitively define the role of GRP78 acetylation in UPR regulation.

Although a primary function of UPR activation is cytoprotective in nature, prolonged pathway activation can lead to cell death signaling.

The balance between these cytoprotective and cell death fates is not well understood at present [16,17]. In our studies, vorinostat induced the expression of CHOP, which is a well-described mediator governing the lethal effects associated with ER stress response. Further, attenuating UPR activation through RNA interference of PERK leads to a significant decrease in vorinostat-induced cytotoxicity, supporting the role this pathway plays in its antitumor activity. However, PERK represents only one of the three central mediators of UPR activation, which also includes ATF6 and inositol-requiring gene 1. Further study involving the influence of vorinostat on these pathways may provide additional insight into the balance of prosurvival and pro–cell death signaling after UPR activation.

References

[1] Baylin SB and Ohm JE (2006). Epigenetic gene silencing in cancer—a mechanism for early oncogenic pathway addiction? *Nat Rev Cancer* **6**, 107–116.

[2] Glozak MA and Seto E (2007). Histone deacetylases and cancer. *Oncogene* **26**, 5420–5432.

[3] Bolden JE, Peart MJ, and Johnstone RW (2006). Anticancer activities of histone deacetylase inhibitors. *Nat Rev Drug Discov* **5**, 769–784.

[4] Xu WS, Parmigiani RB, and Marks PA (2007). Histone deacetylase inhibitors: molecular mechanisms of action. *Oncogene* **26**, 5541–5552.

[5] Yang Y, Zhao Y, Liao W, Yang J, Wu L, Zheng Z, Yu Y, Zhou W, Li L, Feng J, et al. (2009). Acetylation of FoxO1 activates Bim expression to induce apoptosis in response to histone deacetylase inhibitor depsipeptide treatment. *Neoplasia* **11**, 313–324.

[6] Yang YT, Balch C, Kulp SK, Mand MR, Nephew KP, and Chen CS (2009). A rationally designed histone deacetylase inhibitor with distinct antitumor activity against ovarian cancer. *Neoplasia* **11**, 552–563.

[7] Scroggins BT, Robzyk K, Wang D, Marcu MG, Tsutsumi S, Beebe K, Cotter RJ, Felts S, Toft D, Karnitz L, et al. (2007). An acetylation site in the middle domain of HSP90 regulates chaperone function. *Mol Cell* **25**, 151–159.

[8] Bali P, Pranpat M, Bradner J, Balasis M, Fiskus W, Guo F, Rocha K, Kumaraswamy S, Boyapalle S, Atadja P, et al. (2005). Inhibition of histone deacetylase 6 acetylates and disrupts the chaperone function of heat shock protein 90: a novel basis for antileukemia activity of histone deacetylase inhibitors. *J Biol Chem* **280**, 26729–26734.

[9] Kovacs JJ, Murphy PJ, Gaillard S, Zhao X, Wu JT, Nicchitta CV, Yoshida M, Toft DO, Pratt WB, and Yao TP (2005). HDAC6 regulates HSP90 acetylation and chaperone-dependent activation of glucocorticoid receptor. *Mol Cell* **18**, 601–607.

[10] Kaufman RJ (1999). Stress signaling from the lumen of the endoplasmic reticulum: coordination of gene transcriptional and translational controls. *Genes Dev* **13**, 1211–1233.

[11] Ma Y and Hendershot LM (2004). The role of the unfolded protein response in tumour development: friend or foe? *Nat Rev Cancer* **4**, 966–977.

[12] Pyrko P, Schonthal AH, Hofman FM, Chen TC, and Lee AS (2007). The unfolded protein response regulator GRP78/BiP as a novel target for increasing chemosensitivity in malignant gliomas. *Cancer Res* **67**, 9809–9816.

[13] Lee AS (2007). GRP78 induction in cancer: therapeutic and prognostic implications. *Cancer Res* **67**, 3496–3499.

[14] Duvic M, Talpur R, Ni X, Zhang C, Hazarika P, Kelly C, Chiao JH, Reilly JF, Ricker JL, Richon VM, et al. (2007). Phase 2 trial of oral vorinostat (suberoylanilide hydroxamic acid, SAHA) for refractory cutaneous T-cell lymphoma (CTCL). *Blood* **109**, 31–39.

[15] de Haro C, Mendez R, and Santoyo J (1996). The eIF-2α kinases and the control of protein synthesis. *FASEB J* **10**, 1378–1387.

[16] Lin JH, Li H, Yasumura D, Cohen HR, Zhang C, Panning B, Shokat KM, Lavail MM, and Walter P (2007). IRE1 signaling affects cell fate during the unfolded protein response. *Science* **318**, 944–949.

[17] Lin JH, Li H, Zhang Y, Ron D, and Walter P (2009). Divergent effects of PERK and IRE1 signaling on cell viability. *PLoS ONE* **4**, e4170.